Molecular Therapy
Original Article

Targeting of pancreatic cancer cells and stromal cells using engineered oncolytic *Salmonella typhimurium*

Wenzhi Tan,[1] Mai Thi-Quynh Duong,[2] Chaohui Zuo,[3] Yeshan Qin,[2] Ying Zhang,[2] Yanxia Guo,[1] Yeongjin Hong,[4] Jin Hai Zheng,[1,2] and Jung-Joon Min[2,5]

[1]School of Biomedical Sciences, Hunan University, Changsha, Hunan 410082, China; [2]Institute for Molecular Imaging and Theranostics, Chonnam National University Hwasun Hospital, Jeonnam 58128, Republic of Korea; [3]Department of Gastroduodenal and Pancreatic Surgery, Hunan Cancer Hospital, Changsha, Hunan 410013, China; [4]Department of Microbiology, Chonnam National University Medical School, Gwangju 61469, Republic of Korea; [5]Department of Nuclear Medicine, Chonnam National University Hwasun Hospital, Jeonnam 58128, Republic of Korea

Pancreatic cancer is resistant to conventional therapeutic interventions, mainly due to abundant cancer stromal cells and poor immune cell infiltration. Here, we used a targeted cancer therapy approach based on attenuated *Salmonella typhimurium* engineered to express cytolysin A (ClyA) to target cancer stromal cells and cancer cells and treat pancreatic cancer in mice. Nude mice bearing subcutaneous or orthotopic human pancreatic cancers were treated with engineered *S. typhimurium* expressing ClyA. The tumor microenvironment was monitored to analyze stromal cell numbers, stromal cell marker expression, and immune cell infiltration. The attenuated bacteria accumulated and proliferated specifically in tumor tissues after intravenous injection. The bacteria secreted ClyA into the tumor microenvironment. A single dose of ClyA-expressing *Salmonella* markedly inhibited growth of pancreatic cancer both in subcutaneous xenograft- and orthotopic tumor-bearing nude mice. Histological analysis revealed a marked decrease in expression of stromal cell markers and increased immune cell (neutrophils and macrophages) infiltration into tumors after colonization by ClyA-expressing bacteria. ClyA-expressing *S. typhimurium* destroyed cancer stromal cells and cancer cells in mouse models of human pancreatic cancer. This approach provides a novel strategy for combining anticancer and antistromal therapy to treat pancreatic cancer.

INTRODUCTION

Pancreatic ductal adenocarcinoma (PDAC), which covers more than 90% of pancreatic cancer cases and is known simply as pancreatic cancer,[1,2] is a highly aggressive malignancy; indeed, the median survival time following diagnosis is 3–5 months, with a median 5-year survival of 8%.[3,4] PDAC is the fourth leading cause of cancer-related death in Western countries, even though it is only the ninth most common malignancy.[4,5] However, only 20% of patients are suitable for surgical resection when diagnosed at an early stage.[6] The most common chemotherapeutic drugs approved for pancreatic cancer treatment are gemcitabine and 5-fluorouracil (5-FU); however, only modest advances have been made to improve patient outcomes.[6,7] Cancer immunotherapy with checkpoint blockers has shown remarkable responses in some cancers;[8–11] however, they fail to show any efficacy against PDAC,[10,12] even dual or triple combination therapy with a programmed cell death 1 (PD-1) inhibitor (nivolumab), a cytotoxic T lymphocyte-associated protein 4 (CTLA-4) inhibitor (ipilimumab), and a mitogen-activated protein kinase (MEK) inhibitor (cobimetinib).[13] Thus, a new paradigm for therapy is needed if we are to improve the prospects of patients with pancreatic cancer.

Attenuated *Salmonella typhimurium* strains target various types of cancer, including colon cancer,[14,15] cervical cancer,[16] breast cancer,[17,18] and glioma.[19,20] The unique properties of tumor microenvironments (TMEs), such as low oxygen, abundant nutrients released from necrotic cancer cells, immunosuppressive conditions, and chemotaxis, promote bacterial colonization and proliferation in tumor tissues.[21–23] A genetically engineered *S. typhimurium* strain defective in ppGpp synthesis (ΔppGpp) shows an increased 50% lethal dose (LD_{50}) (10,000- to 1,000,000-fold) compared with the wild-type strain.[24] The avirulent ΔppGpp strain (SL) specifically colonizes and proliferates in tumor tissue, thereby recruiting immune cells and inhibiting tumor growth.[14,25,26] To increase the efficacy of this so-called bacterial cancer therapy (BCT), SL was engineered further to express anticancer agents in the TME. Bacterial engineering allows researchers to explore different therapeutic mechanisms. Previously, we engineered SL to express different therapeutic payloads: these include Noxa, a mitochondrial target

Received 4 November 2020; accepted 8 August 2021;
https://doi.org/10.1016/j.ymthe.2021.08.023.

Correspondence: Jung-Joon Min, Institute for Molecular Imaging and Theranostics, Chonnam National University Hwasun Hospital, Jeonnam 58128, Republic of Korea.
E-mail: jjmin@jnu.ac.kr
Correspondence: Jin Hai Zheng, College of Biology, Hunan University, Changsha, Hunan 410082, China.
E-mail: jhzheng@hnu.edu.cn

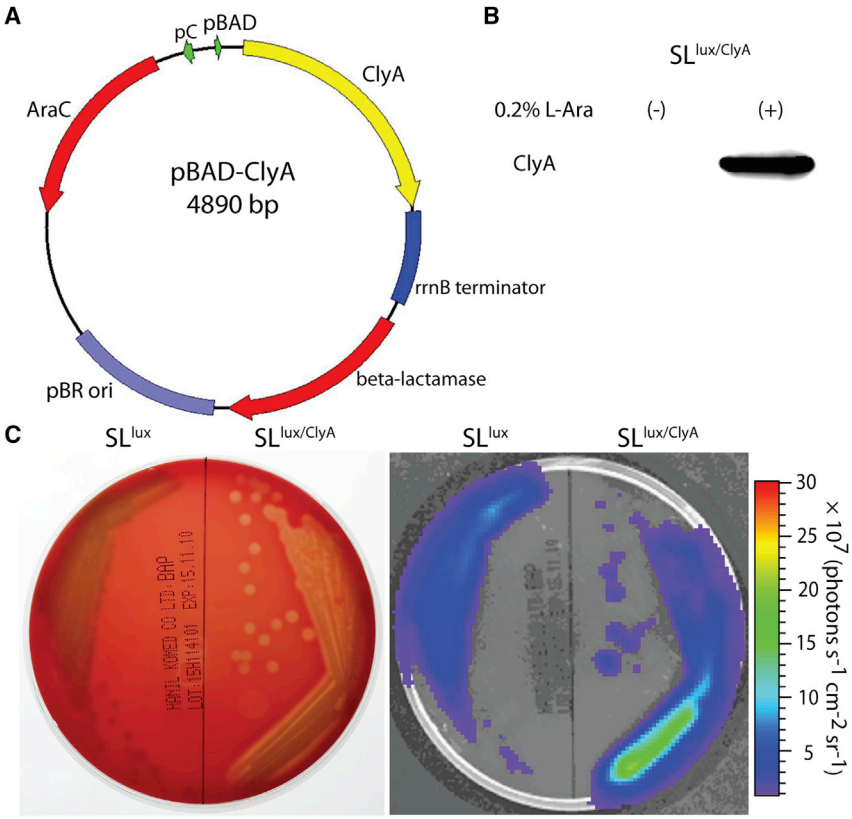

Figure 1. *In vitro* expression of ClyA by engineered *S. typhimurium* carrying the pBAD-ClyA plasmid

(A) Map of the engineered plasmid pBAD-ClyA. (B) The bioluminescent ΔppGpp *Salmonella* (SL^{lux}) strain was transformed with pBAD-ClyA ($SL^{lux/ClyA}$). Expression of ClyA (34 kDa) in bacterial culture was analyzed by western blotting with an anti-ClyA antibody without (–) or with (+) induction with 0.2% L-arabinose. (C) After spreading 100 μL of 40% L-arabinose on the sheep blood, the plates were divided into two parts; the left side was streaked with live SL^{lux}, whereas the right side was streaked with live $SL^{lux/ClyA}$. Then, the plates were incubated at 37°C overnight. Engineered $SL^{lux/ClyA}$ lyses blood cells (left) and produces a clear bioluminescent signal in the corresponding area of hemolysis (right).

domain, that induces cancer cell death by increasing mitochondrial permeability;[27] heterologous bacterial flagellin (FlaB, *Vibrio vulnificus* flagellin B), which modulates anticancer immunity;[15] and cytolysin A (ClyA), a native bacterial toxin from *S. typhimurium* that kills cancer cells and cancer stromal cells via its pore-forming activity.[25,28]

The TME is a complex milieu that contains tumor cells and non-malignant host stromal cells, including blood endothelial cells (BECs), lymphatic endothelial cells (LECs), mesenchymal stem cells, cancer-associated fibroblasts (CAFs), and pericytes.[29,30] These cells secrete inhibitory signals that suppress immune cells and play crucial roles in cancer initiation, progression, and metastasis.[29–31] In particular, PDAC is characterized by a dense fibrous stroma that inhibits drug penetration and immune cell infiltration.[32] Therefore, targeted depletion of cancer stromal cells along with cancer cells would be an effective strategy to manage PDAC.[33]

Here, we used an avirulent SL strain engineered to express ClyA (SL^{ClyA}) to treat PDAC in various mouse models. We demonstrate anticancer effects against subcutaneous xenograft and orthotopic human PDACs, which are thought to be clinically relevant and offer site-specific pathology.[34] The engineered SL^{ClyA} showed specific tumor-targeting ability, destruction of cancer stromal cells and cancer cells, and subsequent inhibition of cancer growth.

RESULTS

Engineering ClyA-producing *Salmonella*

To generate an inducible vector system for bacterial expression of a therapeutic gene, we cloned the *clyA* gene into the pBAD plasmid vector (Figure 1A), as described previously.[28] Western blot analysis revealed that $SL^{lux/ClyA}$ expressed the ClyA protein after L-arabinose induction, whereas no ClyA protein was detected in the absence of L-arabinose (Figure 1B). $SL^{lux/ClyA}$ lysed blood cells and generated a clear bioluminescence signal in areas corresponding to hemolysis (Figure 1C). Furthermore, additional experiments were performed with the AsPC-1 cell line, which showed effective cell killing *in vitro* as confirmed by crystal violet staining and lactate dehydrogenase release assay (Figure S1).

Bacterial distribution and ClyA expression in tumor tissue

We reported previously that systemically injected $SL^{lux/ClyA}$ colonized the liver and spleen initially, but began to proliferate preferentially in tumors at 3 days post-inoculation (dpi) (Figure S2).[15,25] To check selective accumulation and proliferation of bacteria in pancreatic cancer, we administered $SL^{lux/ClyA}$ (3.0×10^7 colony-forming units [CFU]) to BALB/c athymic nu^-/nu^- mice bearing AsPC-1 xenografts via intravenous (i.v.) injection. Normal organs (liver and spleen) and tumor tissues were extracted at 3 dpi, and viable bacteria were counted. We observed a high number of bacteria ($>10^{10}$ CFU/g) in AsPC-1 xenografts; indeed, numbers were 1,000- to 10,000-fold higher than those in the liver and spleen (Figure 2A). The number of bacteria agreed with the results of *in vivo* and *ex vivo* imaging at 3 dpi, which showed specific bioluminescence signals in tumors but not in the liver and spleen (Figures S3 and S4). Therefore, expression of therapeutic genes at this time point should cause minimal, if any, toxicity to normal tissues. Thus, we decided to administer L-arabinose to tumor-bearing mice at 3 dpi.

Next, we examined expression of ClyA in implanted AsPC-1 tumors treated with $SL^{lux/ClyA}$ in the presence of L-arabinose. Control

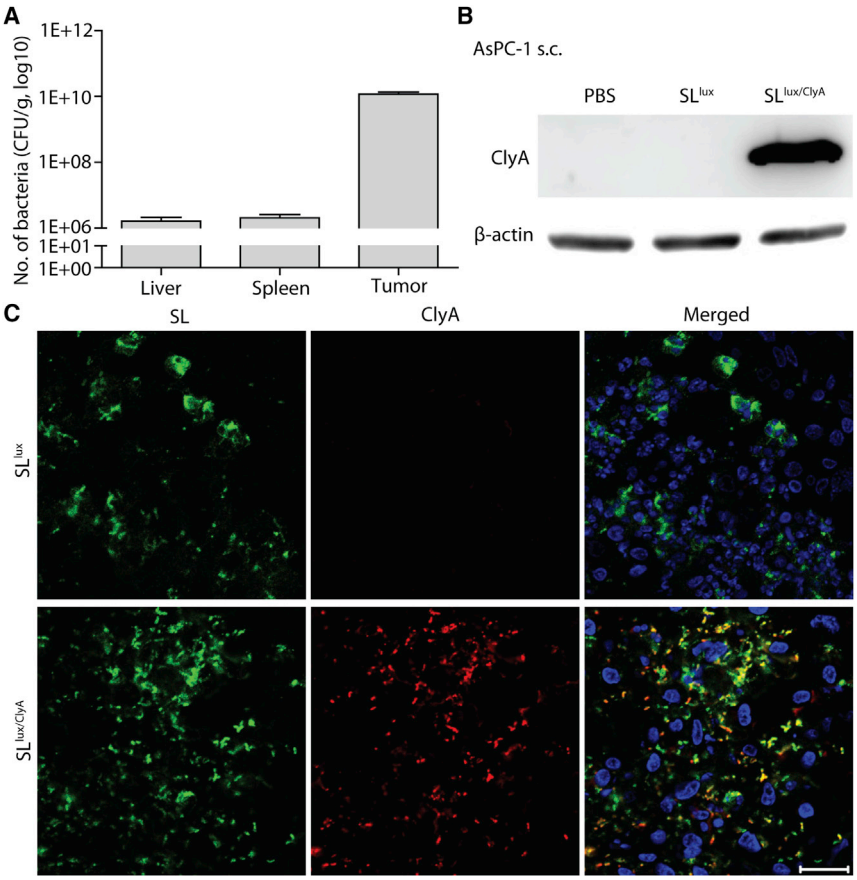

Figure 2. Bacterial colonization and expression of ClyA in AsPC-1 xenografts

BALB/c athymic nu⁻/nu⁻ mice bearing AsPC-1 tumors were injected intravenously with engineered $SL^{lux/ClyA}$ (3.0×10^7 CFU), followed by intraperitoneal injection of L-arabinose (daily, starting at 3 dpi). (A) Viable bacteria in tumors were counted at 3 dpi. Quantification of bacterial numbers in the liver, spleen, and tumor (n = 11 mice) is shown. (B) Western blot analysis of ClyA expression in AsPC-1 tumor tissue from mice injected with engineered SL^{lux} or $SL^{lux/ClyA}$ at 6 h after L-arabinose induction (representative images of three repetitions). (C) Immunofluorescence staining shows bacterial colonization and ClyA expression in AsPC-1 tumor tissues at 6 h after L-arabinose induction. Sections were stained with an anti-*Salmonella* antibody (green), an anti-ClyA antibody (red), and DAPI/antifade (blue). A merged image is shown (Merged). Data are representative of three independent experiments. Scale bar, 20 μm.

experiments used tumors treated with SL^{lux} carrying an empty vector. Western blot analysis of excised AsPC-1 tumor tissues demonstrated expression of ClyA in tumors colonized by $SL^{lux/ClyA}$ exposed to L-arabinose, but not in tumors exposed to PBS or SL^{lux} (Figure 2B). Expression of ClyA in AsPC-1 tumor tissue was further assessed by immunofluorescence staining. Histological analysis revealed abundant bacteria in tumor tissues from *Salmonella*-injected mice. The ClyA protein was detected only in tumor tissues harboring $SL^{lux/ClyA}$ in the presence of L-arabinose (Figure 2C). Taken together, these results confirm that engineered $SL^{lux/ClyA}$ specifically expresses and secretes ClyA in pancreatic cancer tissue.

Anticancer effects of engineered ClyA-secreting *Salmonella* in subcutaneous pancreatic cancer models in nude mice

To evaluate the antitumor effects of engineered *Salmonella*, BALB/c athymic nu⁻/nu⁻ mice were implanted subcutaneously with AsPC-1 or Capan-2 tumors and injected i.v. with PBS, SL^{lux}, or $SL^{lux/ClyA}$ (+L-arabinose induction from 3 dpi). Tumor-bearing mice tolerated treatment with all types of salmonellae. In mice treated with $SL^{lux/ClyA}$ in the presence of L-arabinose, tumor growth was significantly lower than that in the other groups (Figure 3; Figures S5 and S6). At the end of the treatment (45 days after tumor implantation), growth of AsPC-1 treated with $SL^{lux/ClyA}$ was suppressed significantly, whereas the volume of tumors treated with PBS or SL^{lux} increased by 6-fold and 3-fold, respectively (Figures 3A–3D; p (PBS versus SL^{lux}) = 0.0025; p (PBS versus $SL^{lux/ClyA}$) = 0.0002; p (SL^{lux} versus $SL^{lux/ClyA}$) = 0.0006). A similar result was observed in Capan-2-bearing mice. For example, 47 days after tumor implantation, the volume of Capan-2 tumors was 51 ± 14 mm^3 in the group treated with $SL^{lux/ClyA}$, whereas it was 294 ± 20 mm^3 or 147 ± 7 mm^3 in the groups treated with PBS or SL^{lux}, respectively (Figures 3E–3H). These results demonstrate that ClyA-secreting *Salmonella* suppresses cancer growth in subcutaneous human pancreatic cancer models.

Bacterial colonization and anticancer effects in orthotopic pancreatic cancer-bearing nude mice

To further explore the anticancer effects of engineered ClyA-secreting *Salmonella*, we established an orthotopic pancreatic cancer model via surgical implantation of AsPC-1 stably expressing firefly luciferase (AsPC-1/Fluc) (Figure S7A). H&E staining of pancreatic tissues obtained 11 days after surgical orthotopic implantation (SOI) clearly showed cancer development and invasion of cancer cells into normal pancreatic tissue (Figure S7B). Generation and growth of orthotopic pancreatic cancer was observed by bioluminescence imaging (Figure S7C). Changes in bioluminescence activity in an individual mouse are shown in Figure S7D. Histological analysis revealed a poorly differentiated structure of pancreatic adenocarcinoma. Abundant cancer stromal cells were also found by immunofluorescence staining with fibroblast activation protein (FAP) and platelet-derived growth factor receptor β (PDGFRβ), which suggested similar complexity to clinical PDAC patient-derived cancer samples (Figure S8).

BALB/c athymic nu⁻/nu⁻ mice bearing orthotopic pancreatic cancer were injected i.v. with engineered $SL^{lux/ClyA}$ 15 days after SOI. Counting

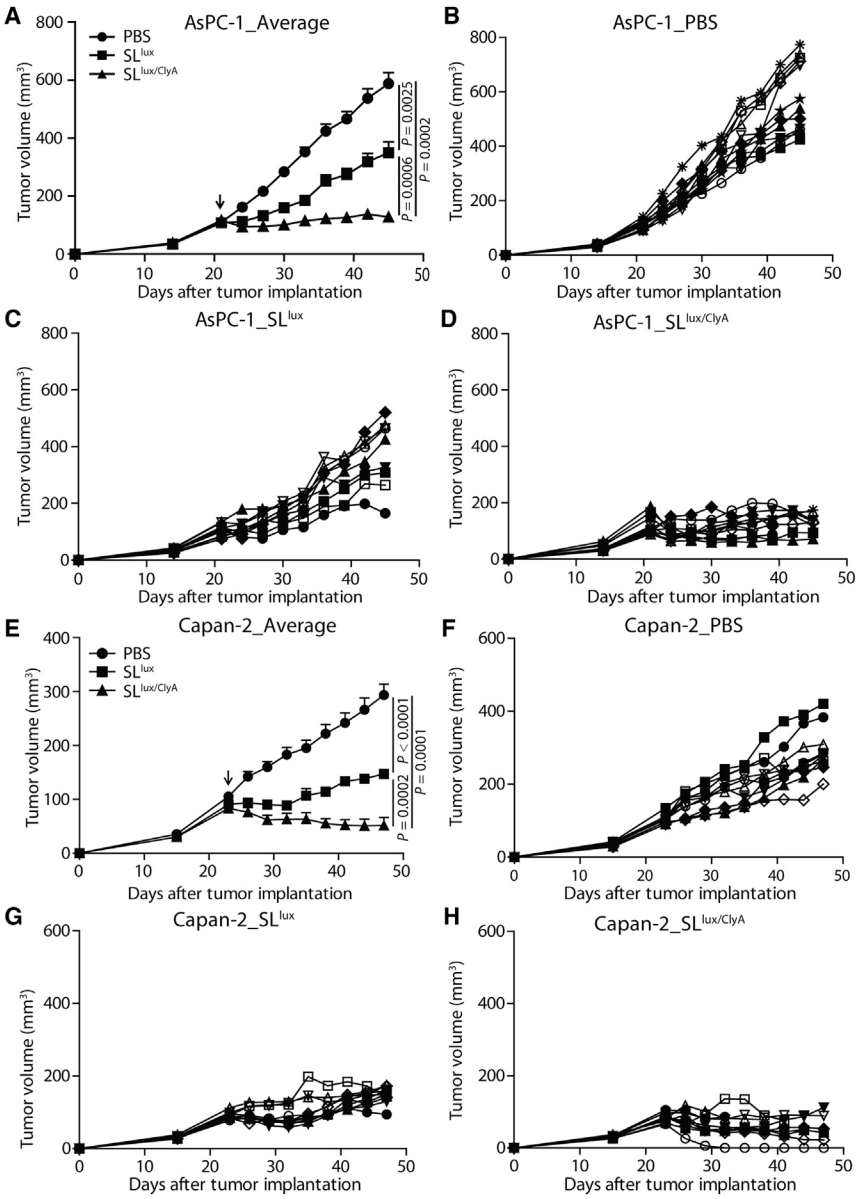

Figure 3. Anticancer effects of engineered ClyA-expressing bacteria in subcutaneous cancer models

Nude mice were implanted subcutaneously with AsPC-1 (A–D, n = 12 mice per group) or Capan-2 (E–H, n = 10 mice per group) cancer cells. When the tumor reached 100–120 mm^3, mice were treated with 3.0×10^7 CFU engineered bacteria (SL^{lux} or $SL^{lux/ClyA}$, indicated by an arrow). (A) Average tumor growth in the AsPC-1 cancer model. (B–D) AsPC-1 tumors were treated with PBS (B), engineered SL^{lux} (C), or $SL^{lux/ClyA}$ (D). (E) Average tumor growth in the Capan-2 cancer model. (F–H) Capan-2 tumors were treated with PBS (F), engineered SL^{lux} (G), or $SL^{lux/ClyA}$ (H).

of viable bacteria at 3, 11, and 20 dpi revealed specific colonization and proliferation in the orthotopic cancer, resulting in >1,000- and 10,000-fold higher numbers of bacteria than in the spleen and liver, respectively (Figure S9A). The number of bacteria in the orthotopic cancers remained high at 3 and 11 dpi ($p = 0.1949$), followed by a gradual decrease (100-fold) until 20 dpi. This suggests that the engineered *Salmonella* can be used as an active vehicle for delivery and expression of anticancer agents in orthotopic pancreatic cancer.

Next, we examined anticancer activity in orthotopic pancreatic cancer models after i.v. injection of PBS, SL, or SL^{ClyA} on day 15 after SOI. As shown in Figure 4A, SL^{ClyA} suppressed pancreatic cancer growth, as demonstrated by bioluminescence imaging of mice bearing orthotopic AsPC-1/Fluc tumors ($p < 0.0001$). Compared with that in the control PBS-treated group (negative control), orthotopic cancer growth was suppressed in mice treated with SL ($p = 0.0004$). The change in bioluminescence activity in orthotopic AsPC-1/Fluc cancers further indicated that SL^{ClyA} mediated robust anticancer effects (Figure 4B). At the end of the experiment (day 35 after SOI), orthotopic pancreatic tumors were excised and weighed. The average weight of primary tumors in the group treated with SL^{ClyA} was significantly lower than that in the group treated with SL (121 ± 21 mg versus 269 ± 16 mg; $p = 0.0079$) or PBS (121 ± 21 mg versus 422 ± 10 mg; $p = 0.0043$) (Figure 4C). These results indicate that SL^{ClyA} inhibits pancreatic cancer growth in an orthotopic human pancreatic cancer model (Figure S9B).

Changes in cancer stromal cells after treatment with ClyA-secreting *Salmonella*

To examine changes in cancer stromal cells after treatment with ClyA-secreting *Salmonella*, we evaluated expression of several stromal cell markers in AsPC-1 before and after treatment with SL^{lux} or $SL^{lux/ClyA}$. Western blot analysis revealed significant reductions in expression of neural/glial antigen 2 (NG2), PDGFRβ, and cluster of differentiation 31 (CD31) after treatment with $SL^{lux/ClyA}$, indicating damaged CAFs, pericytes, and BECs or LECs (Figure S10; Figure 5A; $p < 0.01$). These results were verified by immunofluorescence staining, which revealed a marked reduction in expression of these markers in tumors treated with $SL^{lux/ClyA}$ (Figure 5B). Furthermore, there was marked infiltration of tumor tissue by immune cells such as macrophages and neutrophils ($p < 0.01$) after treatment with $SL^{lux/ClyA}$ or SL^{lux} (Figure 5C). Taken together, the data show that engineered ClyA-secreting *Salmonella* destroys cancer stromal cells and increases immune cell infiltration, thereby mediating robust anticancer activity.

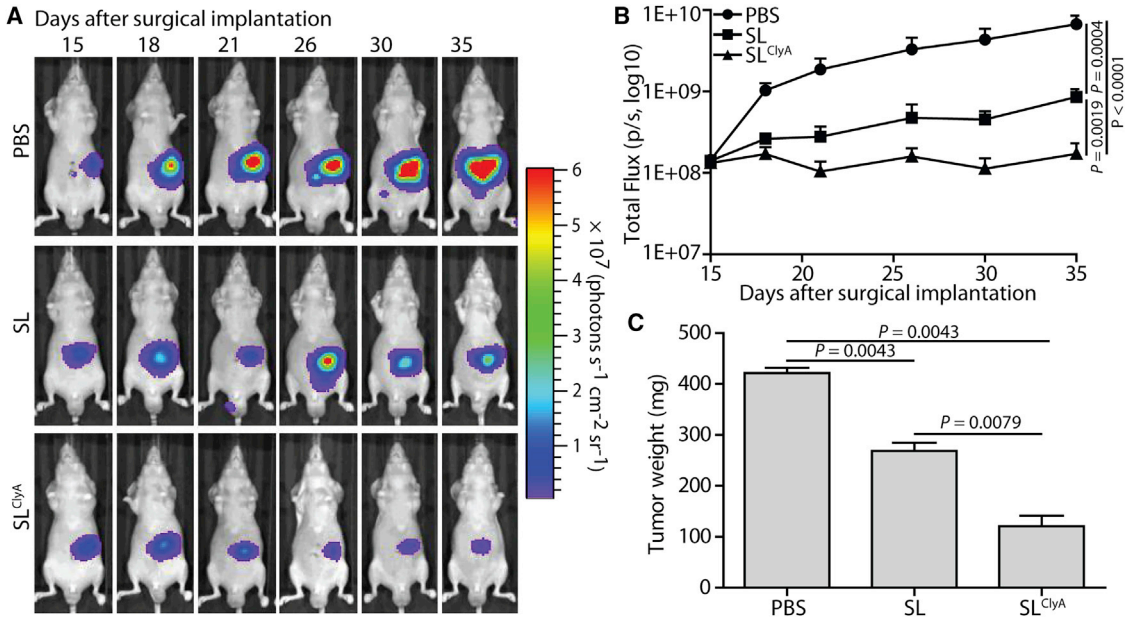

Figure 4. Suppression of orthotopic pancreatic cancer by engineered ClyA-secreting *S. typhimurium*

Orthotopic human pancreatic cancer mouse models (BALB/c nude mice) were generated by surgical orthotopic implantation (SOI) of one 1-mm^3 tumor fragment onto the pancreatic tail. At 15 days after orthotopic implantation, mice were treated with 1.0×10^7 CFU engineered non-light-emitting bacteria (SL or SL^{ClyA}), and tumor development was observed by IVIS imaging (n = 11 mice per group). (A) Changes in the signal generated in tumors from representative mice, as monitored by IVIS. (B) Changes in total flux in tumors, as measured from the day after treatment. (C) Tumor weight at day 35 after surgical implantation.

Anticancer activity against an immunocompetent mouse cancer model

In contrast to T cell immature immunodeficient nude mice, a murine pancreatic cancer model (Pan02) was established in C57BL/6 mice to study anticancer efficacy in an immune-competent host. When the size of tumors reached approximately 120 mm^3, tumor-bearing mice were i.v. injected with PBS, SL^{lux}, or $SL^{lux/ClyA}$ (+L-arabinose induction from 3 dpi). Consistent findings were observed in the Pan02 cancer model compared with AsPC-1 and Capan-2 cancer models. The engineered attenuated bacteria (SL^{lux}) significantly halted cancer growth compared with the PBS-treated control group ($p = 0.0002$), and induction of ClyA expression ($SL^{lux/ClyA}$) further enhanced anticancer efficacy (Figures 6A–6D). By immunofluorescence staining, we monitored the immune cell infiltration and observed increased neutrophil, macrophage, $CD4^+$, and $CD8^+$ T lymphocyte infiltration in tumor tissues (Figures 6E and 6F). Flow cytometry analysis also showed drastically increased immune cell infiltration and activation, with conversion of M2-like macrophages into M1-like macrophages (Figure S11); there was no significant change in immune checkpoints such as PD-1 and CTLA-4 (data not shown). Moreover, ClyA-expressing bacteria significantly promoted the secretion of inflammatory cytokines, such as interleukin (IL)-1β and tumor necrosis factor (TNF)-α (Figure S12). These findings indicated that bacterial therapy exhibited a high potential for TME modification via recruiting a large amount of immune cells and relieving the immunosuppressive conditions.

DISCUSSION

Engineered *Salmonella*-secreting ClyA showed tumor-selective accumulation and drug secretion in mouse models of subcutaneous and orthotopic pancreatic cancer, resulting in marked inhibition of tumor growth. Subsequent induction of ClyA expression altered the TME by destroying cancer stromal cells and cancer cells, which allowed infiltration by immune cells, which may convert non-immunogenic "cold" tumors into immunogenic "hot" tumors. This integrated strategy of microbial delivery of an oncolytic payload represents a new direction for pancreatic cancer management.

BCT has shown some remarkable achievements and has been studied extensively in colon cancer, breast cancer, prostate cancer, lung cancer, and glioma.[15,20,23,35,36] However, BCT of PDAC required further investigation.[37,38] In previous studies, the invasive strain A1-R was applied as an anticancer agent in patient-derived orthotopic xenograft (PDOX) models, showing strong anticancer activity in combination with an anti-angiogenesis agent (bevacizumab) in epidermal growth factor receptor (EGFR)-positive pancreatic cancer,[39] which was comparable to chemotherapies (single drug with 5-FU or gemcitabine).[40] In addition, the PDOX and cell line-based xenografts showed consistent results. Here, we established an orthotopic PDAC model (i.e., AsPC-1/Fluc cell line), which showed similar TME configuration with clinical specimens. We examined the cancer-targeting efficacy of a non-invasive bacterial strain using AsPC-1 xenografts; engineered *S. typhimurium* showed very specific accumulation in tumor tissues when compared with normal organs such as the liver and

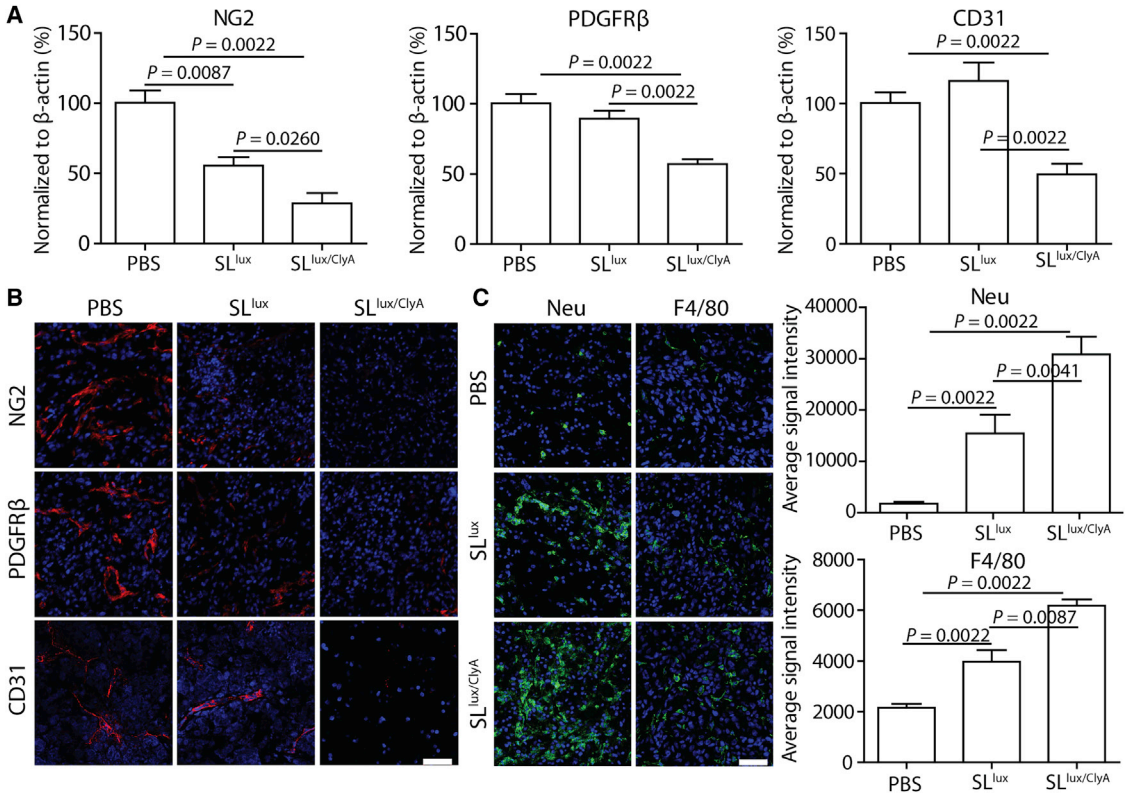

Figure 5. Changes in cancer stromal cells after treatment with ClyA-expressing bacteria

All samples (n = 6 mice per group) were collected from AsPC-1 subcutaneous cancer model mice at 5 days after bacterial infection (3.0×10^7 CFU; 48 h after ClyA induction). (A) Expression of stromal cell markers was analyzed by western blotting; the signal was normalized to that of β-actin (n = 6). (B) Expression of representative markers was confirmed with immunofluorescence staining. NG2, neural/glial antigen 2; PDGFRβ, platelet-derived growth factor receptor β; CD31, cluster of differentiation 31. (C) Immune cell infiltration after treatment with $SL^{lux/ClyA}$ (n = 6). Neu, neutrophil marker; F4/80, macrophage marker. Scale bars, 50 μm.

spleen (1,000- to 10,000-fold higher in tumor tissues), which agrees with our previous reports.[14,15,26] Tumor-selective targeting was observed consistently in an orthotopic PDAC model, which is a more clinically relevant than subcutaneous model in mice; this targeting was maintained at high levels for a long time. The tumor-targeting efficiency of engineered *Salmonella* was supported by the marked regression of PDAC growth in mouse models. The ClyA-secreting *Salmonella* suppressed growth of AsPC-1 and Capan-2 xenografts when compared with controls (*Salmonella* carrying an empty vector). This antitumor activity was reproduced in an orthotopic PDAC model based on AsPC-1. Considering that these results were observed in immunocompromised mice, we speculate that the *Salmonella* engineered to secrete an oncolytic protein (i.e., ClyA) destroys cancer cells directly.[28]

Pancreatic cancer is one of the most stroma-rich cancers; indeed, up to 80% of the tumor mass is made up of stromal tissue.[41] PDAC stroma is highly heterogeneous and comprises pancreatic stellate cells, CAFs, vascular cells, infiltrating immune cells, and an abundant extracellular matrix.[41–43] The stromal cells suppress anticancer immunity by inhibiting immune cell infiltration and by secreting immunosuppressive molecules such as transforming growth factor β (TGF-β), IL-10, and PDGFβ, making the tumor resistant to most chemotherapeutic drugs. Thus, targeted destruction of cancer stroma would be a promising treatment for pancreatic cancer. Preclinical studies targeting PDAC stroma with hyaluronidase to deplete hyaluronic acid showed enhanced drug delivery efficacy, vascular decompression, and stromal remodeling.[44–46] Several representative markers are widely used to dissect cancer stromal cells. For example, NG2 identifies pericytes, which encapsulate the endothelial cells to form blood vessels. CD31 is primarily expressed by BECs, LECs, and some myeloid cells, which can be used for blood vessel staining. PDGFRβ is a marker for CAFs and pericytes.[33] These markers are frequently used for stromal cell studies and are highly expressed in pancreatic cancer tissues. In the present study, bacteria-mediated ClyA secretion in the TME destroyed both cancer stromal cells and cancer cells, thereby facilitating immune cell infiltration of PDAC such as neutrophils, macrophages, and $CD4^+$ and $CD8^+$ T cells as exemplified in the Pan02 cancer model. ClyA secretion further promoted inflammation and immune cell infiltration. The damaged cancer cells were recognized by the host immune system, which then activated adaptive immunity. Given the low immunogenicity and low efficacy of immune checkpoint blockers in

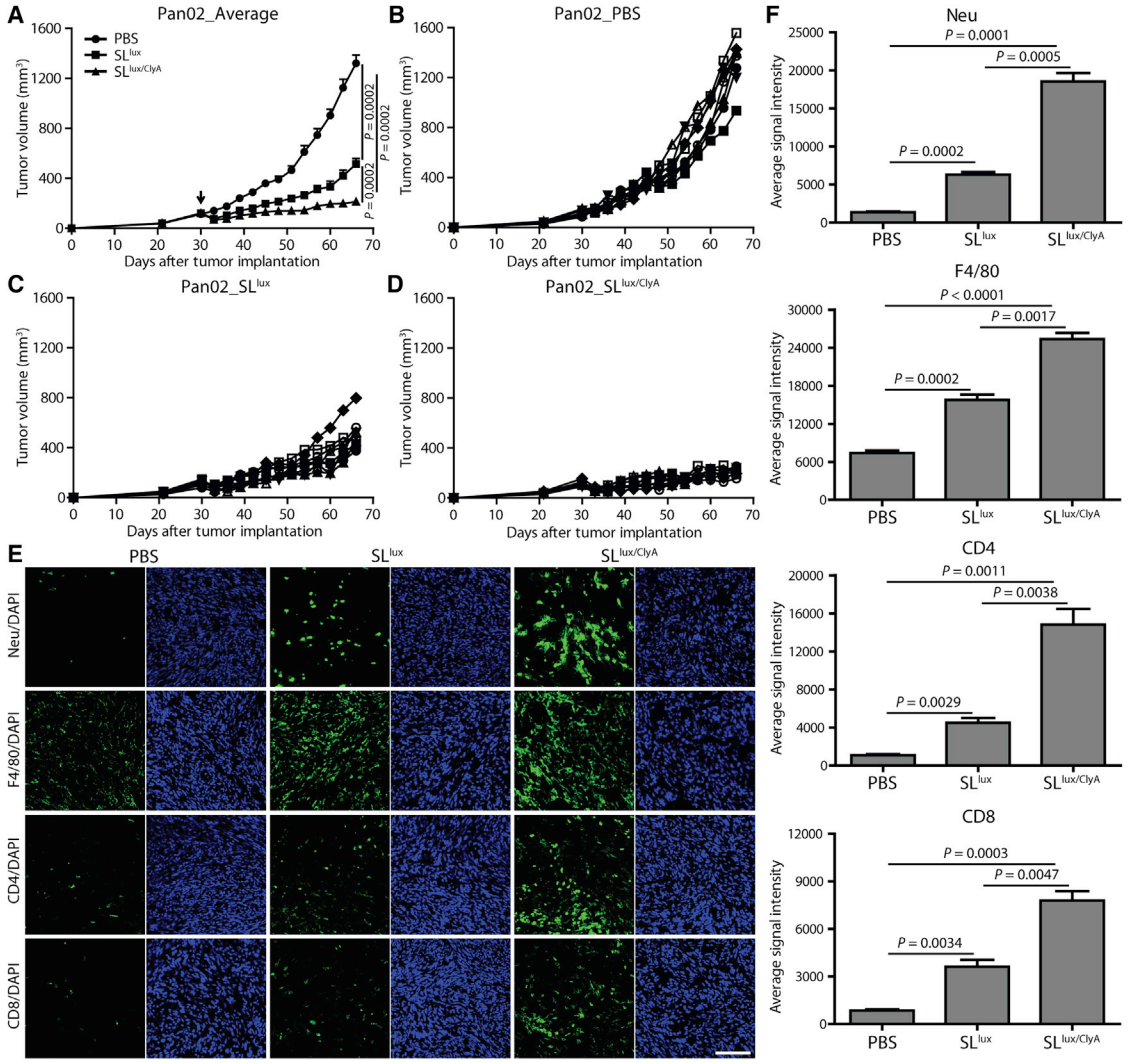

Figure 6. Anticancer activity in the immunocompetent Pan02 murine cancer model

Immune intact C57BL/6 mice were implanted subcutaneously with Pan02 (A–D, n = 8 mice per group) cancer cells. When the tumor reached 100–120 mm^3, mice were treated with 3.0×10^7 CFU engineered bacteria (SL^{lux} or $SL^{lux/ClyA}$, indicated by an arrow). (A) Average tumor growth in the Pan02 cancer model. (B–D) Pan02 tumors were treated with PBS (B), engineered SL^{lux} (C), or $SL^{lux/ClyA}$ (D). (E) Immune cells checked with immunofluorescence staining (n = 3). The average signal intensity was calculated, and results are shown in (F). CD4/CD8, $CD4^+/CD8^+$ T cells. Scale bar, 100 μm.

PDAC, the present approach to modifying the tumor stroma using engineered bacteria producing ClyA would be an effective strategy for treating PDAC.

The therapeutic effect of bacteria is due mainly to their immunomodulatory activity. *Salmonella* infection of tumors may trigger antitumor responses by inducing migration of innate immune cells, including dendritic cells (DCs), neutrophils, macrophages, and neutrophils into colonized tumors, and by enhancing expression of TNF-α, IL-1β, and other pro-inflammatory cytokines.[14,15,26] In addition to the innate immune response, *Salmonella* infection also induces adaptive immune responses against tumor cells by upregulating expression of connexin 43, which promotes the formation of gap junctions between tumor cells and adjacent DCs, enabling transfer of tumor antigens to DCs and cytotoxic T cells.[47] The oncolytic *Salmonella* used in the present study might reproduce this active anticancer immunity in PDAC, an immunologically cold tumor, via destruction of the cancer stroma and by promoting immune cell infiltration. Thus, this study provides a new opportunity for combinational therapies involving immune checkpoint blockades.

In conclusion, genetically engineered bacteria displayed specific tumor colonization in both subcutaneous and orthotopic PDAC with robust anticancer activities by destruction of cancer stromal cells and recruitment of immune cells. Deliberate production of ClyA from the armed bacteria breaks down cancer stromal cells to liberate

the immunosuppressed immune cells and make PDAC more exposed to immunosurveillance. Therefore, targeted cancer therapy with engineered *Salmonella* secreting ClyA is a promising and effective approach to PDAC treatment owing to direct cytotoxicity and immunomodulation through TME remodeling. This programmable strategy based on oncolytic bacteria is a prospective approach to PDAC management in the future.

MATERIALS AND METHODS

Bacterial strains

The *S. typhimurium* strain defective in ppGpp synthesis (*relA::cat, spoT::kan,* SL) has been described previously.[48] The bacterial luciferase gene *lux* was transduced by P22HT *int* transduction.[49] The therapeutic payload, ClyA-encoding plasmid (pBAD-ClyA), has been reported previously.[28] The engineered bacteria was administered to mice via i.v. injection at a dose of 3.0×10^7 CFU for lux-transduced bacteria ($SL^{lux/ClyA}$) or 1.0×10^7 CFU for non-transduced bacteria (SL^{ClyA}). Expression of ClyA was induced by daily intraperitoneal (i.p.) injection of 120 mg of L-arabinose, starting from 3 dpi of bacteria (Table S1).

Cell lines

Human PDAC cell lines AsPC-1 (CRL-1682) and Capan-2 (HTB-80) were obtained from the American Type Culture Collection and authenticated by the Waterborne Virus Bank (Seoul, Korea). The authenticated murine PDAC cell line (Pan02) was purchased from the National Infrastructure of Cell Line Resource (Beijing, China). The cells were maintained at 37°C/5% CO_2 in RPMI 1640, McCoy's 5a modified medium, and DMEM and supplemented with 10% fetal bovine serum and 1% penicillin-streptomycin.

Western blot analysis

Protein concentration was measured using a bicinchoninic acid (BCA) assay (Thermo Scientific, Rockford, IL, USA). Protein samples were separated in 8%–12% sodium dodecyl sulfate-polyacrylamide gels, transferred to nitrocellulose membranes (Bio-Rad, Hercules, CA, USA), and blocked with 5% skim milk for 2 h at room temperature. The membrane was then probed with a primary antibody (Table S2), followed by a horseradish peroxidase-conjugated secondary antibody (Table S2). Immunoreactive proteins were detected using luminol reagents (Santa Cruz Biotechnology, Santa Cruz, CA, USA) and visualized with a Fuji Film image reader (LAS-3000; Fuji Film, Tokyo, Japan).

Animal models

Male BALB/c athymic nu^-/nu^- mice (6–8 weeks old [18–25 g)]) were purchased from the Orient Company (Seongnan, Korea), and female C57BL/6 mice were purchased from the Hunan SJA Laboratory Animal Company (Changsha, China). All experiments and euthanasia procedures were performed in accordance with protocols approved by the Chonnam National University Animal Research Committee (Gwangju, Korea) and Hunan University Animal Research Committee (Changsha, China). Mice were anesthetized with 2% isoflurane (for tumor assessment) or a mixture of ketamine (200 mg/kg) and xylazine (10 mg/kg) (for surgery). AsPC-1 (5×10^6), Capan-2 (5×10^6), and Pan02 (3×10^6) cells were individually implanted subcutaneously into the right flank to generate the mouse cancer models. Tumors were measured with a caliper every 3 days. Tumor volume (mm^3) was calculated using the following formula: $(L \times H \times W)/2$, where L is the length, W is the width, and H is the height of the tumor in millimeters. Treatments were initiated when the tumor size reached around 120 mm^3.

To establish an orthotopic human pancreatic cancer model, tumor fragments were implanted onto the pancreatic tail of BALB/c athymic nu^-/nu^- mice using a SOI method. First, 5×10^6 AsPC-1 cells stably expressing firefly luciferase (AsPC-1/Fluc) were injected subcutaneously into BALB/c athymic nu^-/nu^- mice. When tumors reached 1 cm in diameter, they were excised and the necrotic area was removed. Next, viable tumors were minced into 1-mm^3 pieces prior to surgical transplantation. Recipient animals were anesthetized and a laparotomy was performed. One tumor fragment was implanted orthotopically onto the pancreatic tail of each mouse using an 8-0 surgical suture. The abdominal wall was then closed with a 7-0 surgical suture and the animals were kept in a sterile environment.

Viable bacterial counts

To quantify bacteria-specific colonization and proliferation, tumor tissues and organs (liver and spleen) of engineered $SL^{lux/ClyA}$-infected mice were excised and homogenized in PBS. Samples were serially diluted (10-fold) and plated onto ampicillin/kanamycin-containing Luria-Bertani (LB) plates. After overnight incubation at 37°C, the bacterial titer (CFU/g tissue) was determined by counting the colonies and calculating with the corresponding dilution factor and tissue weight.

Immunofluorescence analysis

For immunofluorescence analysis, tumor tissues were collected from mice and fixed in 4% paraformaldehyde for 2 h at 4°C. The tissues were then washed in PBS, transferred to a 30% sucrose solution, and incubated overnight at 4°C. Fixed tissues were embedded in OCT compound and kept at −80°C. Samples were then sectioned (6 μm thick) using a cryomicrotome (Thermo Scientific, Kalamazoo, MI, USA) and mounted on glass slides. The slides were blocked with 5% BSA and then incubated with primary antibodies overnight at 4°C. The sections were then washed and incubated with fluorochrome-conjugated secondary antibodies for 1 h at room temperature. After counterstaining with DAPI (1:10,000, Invitrogen), the sections were mounted in the ProLong antifade mounting solution (Invitrogen), examined under an LSM510 fluorescence microscope (Zeiss, Germany), and processed using LSM image software.

Optical bioluminescence imaging

Bioluminescence imaging of tumors was performed using an *in vivo* imaging system (IVIS 100; Caliper Life Sciences). Establishment of orthotopic pancreatic cancer was assessed after i.p. injection of 750 μg D-luciferin, as described previously.[28]

Statistical analysis

Statistical analysis was performed using GraphPad Prism 5.0. The Mann-Whitney U test was used to determine the statistical significance of differences in tumor growth, tumor weight, and tumor total flux between the control and treatment groups. A p value <0.05 was considered statistically significant. All data are expressed as the mean ± SEM.

SUPPLEMENTAL INFORMATION

Supplemental information can be found online at https://doi.org/10.1016/j.ymthe.2021.08.023.

ACKNOWLEDGMENTS

This work was supported by the National Research Foundation of Korea (NRF) (grant NRF-2020M3A9G3080282), the Pioneer Research Center Program (2015M3C1A3056410), and the Bio & Medical Technology Development Program of the NRF, funded by the Korean government (MSIT) (NRF-2018M3A9H3024850). W.T. was supported by the National Natural Science Foundation of China (no. 82001753) and the Postdoctoral Science Foundation of China (no. 2020M682562). J.H.Z. was supported by the Hunan Natural Science Foundation (no. 2020JJ5094) and the Fundamental Research Funds for the Central Universities, China. Y.H. was supported by an NRF of Korea grant, funded by the MSIT (no. 2018R1A5A2024181).

AUTHOR CONTRIBUTIONS

W.T. performed the experiments, analyzed the data, drafted the figures, and co-wrote the manuscript. M.T.-Q.D. developed and performed immunofluorescence staining. C.Z., Y.Q., Y.Z., and Y.G. assisted with the animal experiments. Y.H. analyzed and discussed the data. J.H.Z. and J.-J.M. conceived the study, supervised the experiments, analyzed the data, and co-wrote the manuscript.

DECLARATION OF INTERESTS

The authors declare no competing interests.

REFERENCES

1. Bahrami, A., Khazaei, M., Bagherieh, F., Ghayour-Mobarhan, M., Maftouh, M., Hassanian, S.M., et al. (2017). Targeted stroma in pancreatic cancer: Promises and failures of target therapies. J. Cell. Physiol. *232*, 2931–2937.

2. Kleeff, J., Korc, M., Apte, M., La Vecchia, C., Johnson, C.D., Biankin, A.V., Neale, R.E., Tempero, M., Tuveson, D.A., Hruban, R.H., and Neoptolemos, J.P. (2016). Pancreatic cancer. Nat. Rev. Dis. Primers *2*, 16022.

3. Buscail, L., Bournet, B., and Cordelier, P. (2020). Role of oncogenic KRAS in the diagnosis, prognosis and treatment of pancreatic cancer. Nat. Rev. Gastroenterol. Hepatol. *17*, 153–168.

4. Siegel, R.L., Miller, K.D., Fuchs, H.E., and Jemal, A. (2021). Cancer statistics, 2021. CA Cancer J. Clin. *71*, 7–33.

5. Neoptolemos, J.P., Kleeff, J., Michl, P., Costello, E., Greenhalf, W., and Palmer, D.H. (2018). Therapeutic developments in pancreatic cancer: Current and future perspectives. Nat. Rev. Gastroenterol. Hepatol. *15*, 333–348.

6. Karanikas, M., Esempidis, A., Chasan, Z.T., Deftereou, T., Antonopoulou, M., Bozali, F., Amarantidis, K., and Man, Y.G. (2016). Pancreatic cancer from molecular pathways to treatment opinion. J. Cancer *7*, 1328–1339.

7. Mohammed, A., Janakiram, N.B., Pant, S., and Rao, C.V. (2015). Molecular targeted intervention for pancreatic cancer. Cancers (Basel) *7*, 1499–1542.

8. Kvistborg, P., Philips, D., Kelderman, S., Hageman, L., Ottensmeier, C., Joseph-Pietras, D., Welters, M.J., van der Burg, S., Kapiteijn, E., Michielin, O., et al. (2014). Anti-CTLA-4 therapy broadens the melanoma-reactive $CD8^+$ T cell response. Sci. Transl. Med. *6*, 254ra128.

9. Topalian, S.L., Hodi, F.S., Brahmer, J.R., Gettinger, S.N., Smith, D.C., McDermott, D.F., Powderly, J.D., Carvajal, R.D., Sosman, J.A., Atkins, M.B., et al. (2012). Safety, activity, and immune correlates of anti-PD-1 antibody in cancer. N. Engl. J. Med. *366*, 2443–2454.

10. Brahmer, J.R., Tykodi, S.S., Chow, L.Q., Hwu, W.J., Topalian, S.L., Hwu, P., Drake, C.G., Camacho, L.H., Kauh, J., Odunsi, K., et al. (2012). Safety and activity of anti-PD-L1 antibody in patients with advanced cancer. N. Engl. J. Med. *366*, 2455–2465.

11. Powles, T., Eder, J.P., Fine, G.D., Braiteh, F.S., Loriot, Y., Cruz, C., Bellmunt, J., Burris, H.A., Petrylak, D.P., Teng, S.L., et al. (2014). MPDL3280A (anti-PD-L1) treatment leads to clinical activity in metastatic bladder cancer. Nature *515*, 558–562.

12. Royal, R.E., Levy, C., Turner, K., Mathur, A., Hughes, M., Kammula, U.S., Sherry, R.M., Topalian, S.L., Yang, J.C., Lowy, I., and Rosenberg, S.A. (2010). Phase 2 trial of single agent ipilimumab (anti-CTLA-4) for locally advanced or metastatic pancreatic adenocarcinoma. J. Immunother. *33*, 828–833.

13. Leinwand, J., and Miller, G. (2020). Regulation and modulation of antitumor immunity in pancreatic cancer. Nat. Immunol. *21*, 1152–1159.

14. Kim, J.E., Phan, T.X., Nguyen, V.H., Dinh-Vu, H.V., Zheng, J.H., Yun, M., Park, S.G., Hong, Y., Choy, H.E., Szardenings, M., et al. (2015). Salmonella typhimurium suppresses tumor growth via the pro-inflammatory cytokine interleukin-1β. Theranostics *5*, 1328–1342.

15. Zheng, J.H., Nguyen, V.H., Jiang, S.N., Park, S.H., Tan, W., Hong, S.H., Shin, M.G., Chung, I.J., Hong, Y., Bom, H.S., et al. (2017). Two-step enhanced cancer immunotherapy with engineered *Salmonella typhimurium* secreting heterologous flagellin. Sci. Transl. Med. *9*, eaak9537.

16. Hiroshima, Y., Zhang, Y., Zhao, M., Zhang, N., Murakami, T., Maawy, A., Mii, S., Uehara, F., Yamamoto, M., Miwa, S., et al. (2015). Tumor-targeting *Salmonella typhimurium* A1-R in combination with trastuzumab eradicates HER-2-positive cervical cancer cells in patient-derived mouse models. PLoS ONE *10*, e0120358.

17. Ganai, S., Arenas, R.B., and Forbes, N.S. (2009). Tumour-targeted delivery of TRAIL using *Salmonella typhimurium* enhances breast cancer survival in mice. Br. J. Cancer *101*, 1683–1691.

18. Zhao, M., Yang, M., Ma, H., Li, X., Tan, X., Li, S., Yang, Z., and Hoffman, R.M. (2006). Targeted therapy with a *Salmonella typhimurium* leucine-arginine auxotroph cures orthotopic human breast tumors in nude mice. Cancer Res. *66*, 7647–7652.

19. Momiyama, M., Zhao, M., Kimura, H., Tran, B., Chishima, T., Bouvet, M., Endo, I., and Hoffman, R.M. (2012). Inhibition and eradication of human glioma with tumor-targeting *Salmonella typhimurium* in an orthotopic nude-mouse model. Cell Cycle *11*, 628–632.

20. Wen, M., Zheng, J.H., Choi, J.M., Pei, J., Li, C.H., Li, S.Y., Kim, I.Y., Lim, S.H., Jung, T.Y., Moon, K.S., et al. (2018). Genetically-engineered *Salmonella typhimurium* expressing TIMP-2 as a therapeutic intervention in an orthotopic glioma mouse model. Cancer Lett. *433*, 140–146.

21. Guo, Y., Chen, Y., Liu, X., Min, J.J., Tan, W., and Zheng, J.H. (2020). Targeted cancer immunotherapy with genetically engineered oncolytic *Salmonella typhimurium*. Cancer Lett. *469*, 102–110.

22. Kasinskas, R.W., and Forbes, N.S. (2007). *Salmonella typhimurium* lacking ribose chemoreceptors localize in tumor quiescence and induce apoptosis. Cancer Res. *67*, 3201–3209.

23. Zhou, S., Gravekamp, C., Bermudes, D., and Liu, K. (2018). Tumour-targeting bacteria engineered to fight cancer. Nat. Rev. Cancer *18*, 727–743.

24. Na, H.S., Kim, H.J., Lee, H.C., Hong, Y., Rhee, J.H., and Choy, H.E. (2006). Immune response induced by *Salmonella typhimurium* defective in ppGpp synthesis. Vaccine *24*, 2027–2034.

25. Jiang, S.N., Park, S.H., Lee, H.J., Zheng, J.H., Kim, H.S., Bom, H.S., Hong, Y., Szardenings, M., Shin, M.G., Kim, S.C., et al. (2013). Engineering of bacteria for the visualization of targeted delivery of a cytolytic anticancer agent. Mol. Ther. *21*, 1985–1995.

26. Phan, T.X., Nguyen, V.H., Duong, M.T., Hong, Y., Choy, H.E., and Min, J.J. (2015). Activation of inflammasome by attenuated *Salmonella typhimurium* in bacteria-mediated cancer therapy. Microbiol. Immunol. *59*, 664–675.

27. Jeong, J.H., Kim, K., Lim, D., Jeong, K., Hong, Y., Nguyen, V.H., Kim, T.H., Ryu, S., Lim, J.A., Kim, J.I., et al. (2014). Anti-tumoral effect of the mitochondrial target domain of Noxa delivered by an engineered *Salmonella typhimurium*. PLoS ONE *9*, e80050.

28. Nguyen, V.H., Kim, H.S., Ha, J.M., Hong, Y., Choy, H.E., and Min, J.J. (2010). Genetically engineered *Salmonella typhimurium* as an imageable therapeutic probe for cancer. Cancer Res. *70*, 18–23.

29. Mao, Y., Keller, E.T., Garfield, D.H., Shen, K., and Wang, J. (2013). Stromal cells in tumor microenvironment and breast cancer. Cancer Metastasis Rev. *32*, 303–315.

30. Turley, S.J., Cremasco, V., and Astarita, J.L. (2015). Immunological hallmarks of stromal cells in the tumour microenvironment. Nat. Rev. Immunol. *15*, 669–682.

31. Kim, H.M., Jung, W.H., and Koo, J.S. (2015). Expression of cancer-associated fibroblast related proteins in metastatic breast cancer: An immunohistochemical analysis. J. Transl. Med. *13*, 222.

32. Waghray, M., Yalamanchili, M., di Magliano, M.P., and Simeone, D.M. (2013). Deciphering the role of stroma in pancreatic cancer. Curr. Opin. Gastroenterol. *29*, 537–543.

33. Lampi, M.C., and Reinhart-King, C.A. (2018). Targeting extracellular matrix stiffness to attenuate disease: From molecular mechanisms to clinical trials. Sci. Transl. Med. *10*, eaao0475.

34. Qiu, W., and Su, G.H. (2013). Development of orthotopic pancreatic tumor mouse models. Methods Mol. Biol. *980*, 215–223.

35. Hiroshima, Y., Zhang, Y., Murakami, T., Maawy, A., Miwa, S., Yamamoto, M., Yano, S., Sato, S., Momiyama, M., Mori, R., et al. (2014). Efficacy of tumor-targeting *Salmonella typhimurium* A1-R in combination with anti-angiogenesis therapy on a pancreatic cancer patient-derived orthotopic xenograft (PDOX) and cell line mouse models. Oncotarget *5*, 12346–12357.

36. Hiroshima, Y., Zhao, M., Maawy, A., Zhang, Y., Katz, M.H., Fleming, J.B., Uehara, F., Miwa, S., Yano, S., Momiyama, M., et al. (2014). Efficacy of *Salmonella typhimurium* A1-R versus chemotherapy on a pancreatic cancer patient-derived orthotopic xenograft (PDOX). J. Cell. Biochem. *115*, 1254–1261.

37. Park, S.H., Zheng, J.H., Nguyen, V.H., Jiang, S.N., Kim, D.Y., Szardenings, M., Min, J.H., Hong, Y., Choy, H.E., and Min, J.J. (2016). RGD peptide cell-surface display enhances the targeting and therapeutic efficacy of attenuated *Salmonella*-mediated cancer therapy. Theranostics *6*, 1672–1682.

38. Choe, E., Kazmierczak, R.A., and Eisenstark, A. (2014). Phenotypic evolution of therapeutic *Salmonella enterica* serovar Typhimurium after invasion of TRAMP mouse prostate tumor. MBio *5*, e01182-14.

39. Manuel, E.R., Chen, J., D'Apuzzo, M., Lampa, M.G., Kaltcheva, T.I., Thompson, C.B., Ludwig, T., Chung, V., and Diamond, D.J. (2015). *Salmonella*-based therapy targeting indoleamine 2,3-dioxygenase coupled with enzymatic depletion of tumor hyaluronan induces complete regression of aggressive pancreatic tumors. Cancer Immunol. Res. *3*, 1096–1107.

40. Hiroshima, Y., Zhao, M., Zhang, Y., Maawy, A., Hassanein, M.K., Uehara, F., Miwa, S., Yano, S., Momiyama, M., Suetsugu, A., et al. (2013). Comparison of efficacy of *Salmonella typhimurium* A1-R and chemotherapy on stem-like and non-stem human pancreatic cancer cells. Cell Cycle *12*, 2774–2780.

41. Cui, R., Yue, W., Lattime, E.C., Stein, M.N., Xu, Q., and Tan, X.L. (2016). Targeting tumor-associated macrophages to combat pancreatic cancer. Oncotarget *7*, 50735–50754.

42. Apte, M.V., Park, S., Phillips, P.A., Santucci, N., Goldstein, D., Kumar, R.K., Ramm, G.A., Buchler, M., Friess, H., McCarroll, J.A., et al. (2004). Desmoplastic reaction in pancreatic cancer: Role of pancreatic stellate cells. Pancreas *29*, 179–187.

43. Mei, L., Du, W., and Ma, W.W. (2016). Targeting stromal microenvironment in pancreatic ductal adenocarcinoma: controversies and promises. J. Gastrointest. Oncol. *7*, 487–494.

44. Jacobetz, M.A., Chan, D.S., Neesse, A., Bapiro, T.E., Cook, N., Frese, K.K., Feig, C., Nakagawa, T., Caldwell, M.E., Zecchini, H.I., et al. (2013). Hyaluronan impairs vascular function and drug delivery in a mouse model of pancreatic cancer. Gut *62*, 112–120.

45. Provenzano, P.P., Cuevas, C., Chang, A.E., Goel, V.K., Von Hoff, D.D., and Hingorani, S.R. (2012). Enzymatic targeting of the stroma ablates physical barriers to treatment of pancreatic ductal adenocarcinoma. Cancer Cell *21*, 418–429.

46. Thompson, C.B., Shepard, H.M., O'Connor, P.M., Kadhim, S., Jiang, P., Osgood, R.J., Bookbinder, L.H., Li, X., Sugarman, B.J., Connor, R.J., et al. (2010). Enzymatic depletion of tumor hyaluronan induces antitumor responses in preclinical animal models. Mol. Cancer Ther. *9*, 3052–3064.

47. Saccheri, F., Pozzi, C., Avogadri, F., Barozzi, S., Faretta, M., Fusi, P., and Rescigno, M. (2010). Bacteria-induced gap junctions in tumors favor antigen cross-presentation and antitumor immunity. Sci. Transl. Med. *2*, 44ra57.

48. Song, M., Kim, H.J., Kim, E.Y., Shin, M., Lee, H.C., Hong, Y., Rhee, J.H., Yoon, H., Ryu, S., Lim, S., and Choy, H.E. (2004). ppGpp-dependent stationary phase induction of genes on *Salmonella* pathogenicity island 1. J. Biol. Chem. *279*, 34183–34190.

49. Davis, R.W., Botstein, D., and Roth, J.R. (1980). Advanced Bacterial Genetics: A Manual for Genetic Engineering (Cold Spring Harbor Laboratory Press).

YMTHE, Volume *30*

Supplemental Information

Targeting of pancreatic cancer cells and stromal cells using engineered oncolytic *Salmonella typhimurium*

Wenzhi Tan, Mai Thi-Quynh Duong, Chaohui Zuo, Yeshan Qin, Ying Zhang, Yanxia Guo, Yeongjin Hong, Jin Hai Zheng, and Jung-Joon Min

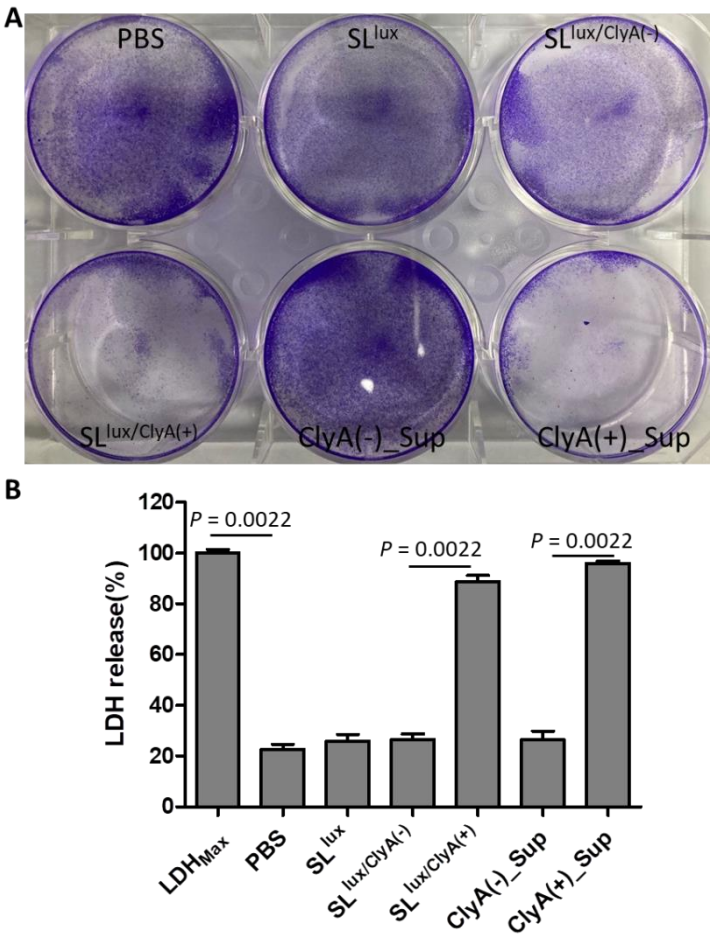

Figure S1. In vitro cell killing of AsPC-1 by ClyA-expressing bacteria. 1×10^6 cell/well were seeded in a 6-well plate, and after 24 h, the cells were co-cultured with 100 MOI (multiplicity of infection, bacteria: cell = 100:1) SL^{lux} and $SL^{lux/ClyA}$ with or without 8 h induction of 0.2% L-arabinose. 120 μg/ml of gentamycin was subsequently added into the culture, and the culture was maintained for another 36 h. Bacteria culture supernatant (Sup) collected from $SL^{lux/ClyA}$ with or without 8 h induction of 0.2% L-arabinose was also added to the cells as shown in the last two wells at a final concentration of 15% (v/v). (A) The plate was stained with crystal violet after 36 h treatment. (B) Lactate dehydrogenase (LDH) release was measured in the cell-culture supernatant. Completely lysed cells served as the positive control (LDH_{Max}, n = 6).

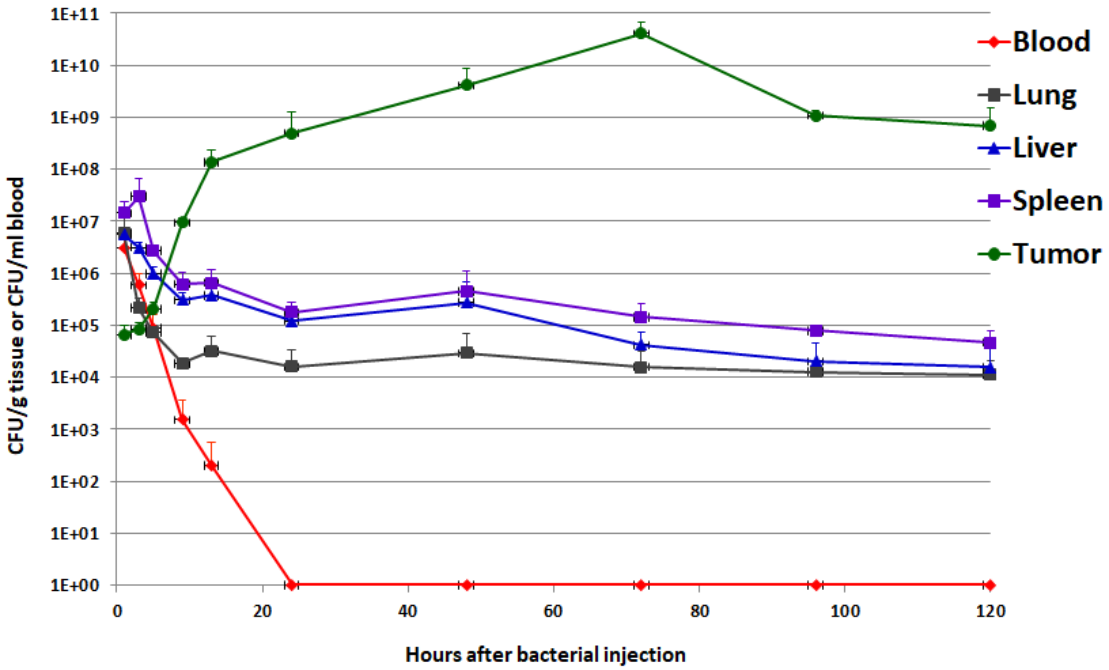

Figure S2. Bacterial biodistribution in vivo. Attenuated bacteria have broad and very specific targeting abilities toward various kinds of solid tumors, and the MC38 murine colon cancer in immunocompetent C57BL/6 mice was applied to. Samples were collected from MC38 tumor-bearing mice at indicated time points post-bacterial infection. Viable bacterial numbers were quantified with colony counts to study the biodistribution of attenuated *Salmonella typhimurium* (SL) in vivo (n = 11).

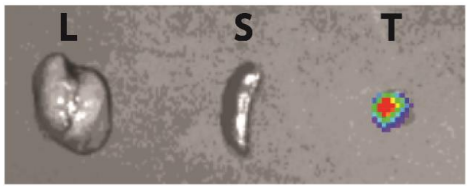

Figure S3. Ex vivo imaging of AsPC-1 xenografts post-bacterial injection. AsPC-1 (n = 11 mice per group) cancer model mice were treated with engineered $SL^{lux/ClyA}$. When the tumor reached 100–120 mm^3, mice were treated with 3.0×10^7 CFU engineered bacteria. Bacterial bioluminescence, as monitored by IVIS imaging, at 3 dpi. L: liver, S: spleen, T: tumor.

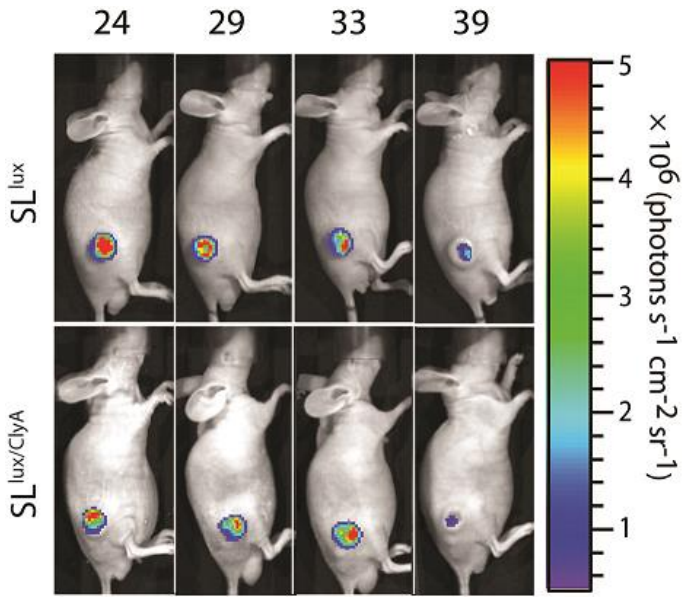

Figure S4. Bacterial colonization of AsPC-1 subcutaneous tumors. AsPC-1 (n = 12 mice per group) cancer model mice were treated with engineered *Salmonella*. When the tumors reached 100–120 mm^3, mice were treated with 3.0×10^7 CFU engineered SL^{lux} or $SL^{lux/ClyA}$. Bacterial bioluminescence, as monitored by IVIS imaging, in a representative mouse from each group.

Figure S5. Photographs of representative AsPC-1 cancer model mice. AsPC-1 (n = 12 mice per group) cancer model mice were treated with PBS, engineered SL^{lux}, or $SL^{lux/ClyA}$. When the tumor reached 100–120 mm^3, mice were treated with 3.0×10^7 CFU engineered bacteria. Representative photos from each group are shown.

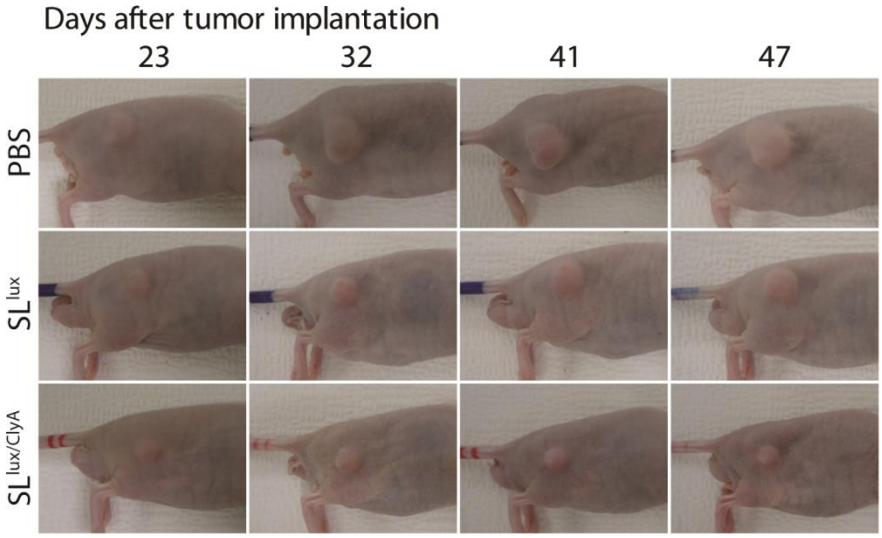

Figure S6. Photographs of representative Capan-2 cancer model mice. Capan-2 (n = 10 mice per group) cancer model mice were treated with PBS, engineered SL^{lux}, or $SL^{lux/ClyA}$. When the tumor reached 100–120 mm^3, mice were treated with 3.0×10^7 CFU engineered bacteria. Representative photos from each group are shown.

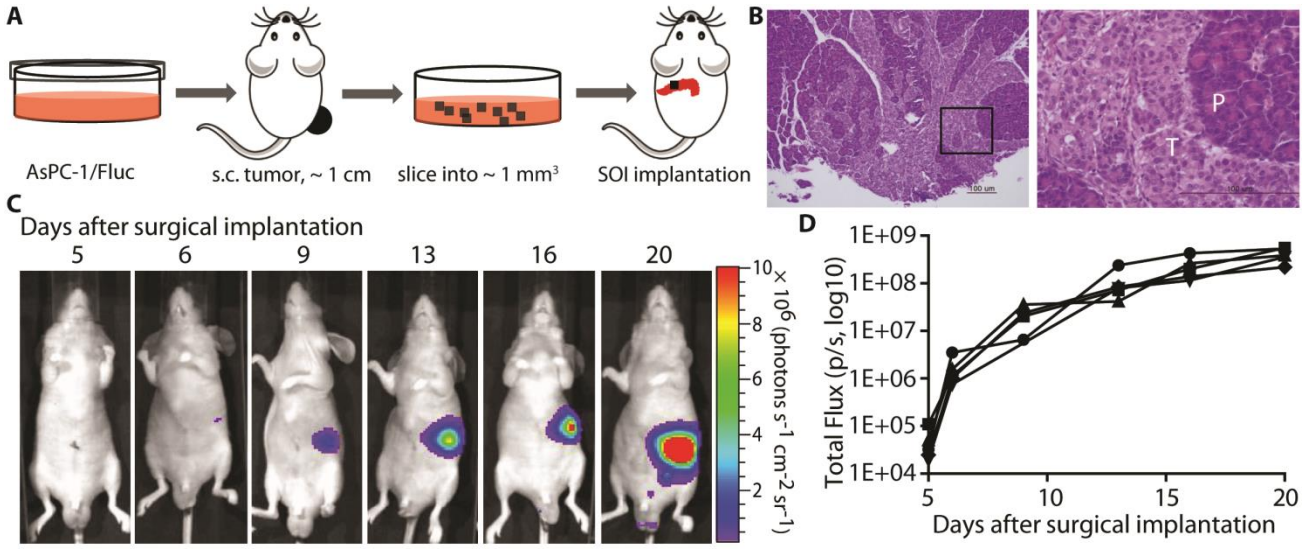

Figure S7. Generation of an orthotopic pancreatic cancer model in nude mice. (A) Schematic showing the generation of an orthotopic pancreatic cancer model. (B) Confirmation of local tumor invasion (Day 11) into normal pancreatic tissue (H&E staining; n = 6 mice). Scale bar = 100 μm. (C) Representative bioluminescence images showing developmental dynamics of orthotopic pancreatic cancer (AsPC-1/Fluc), as monitored by IVIS. (D) Changes in tumor total Flux in individual mouse (n = 5).

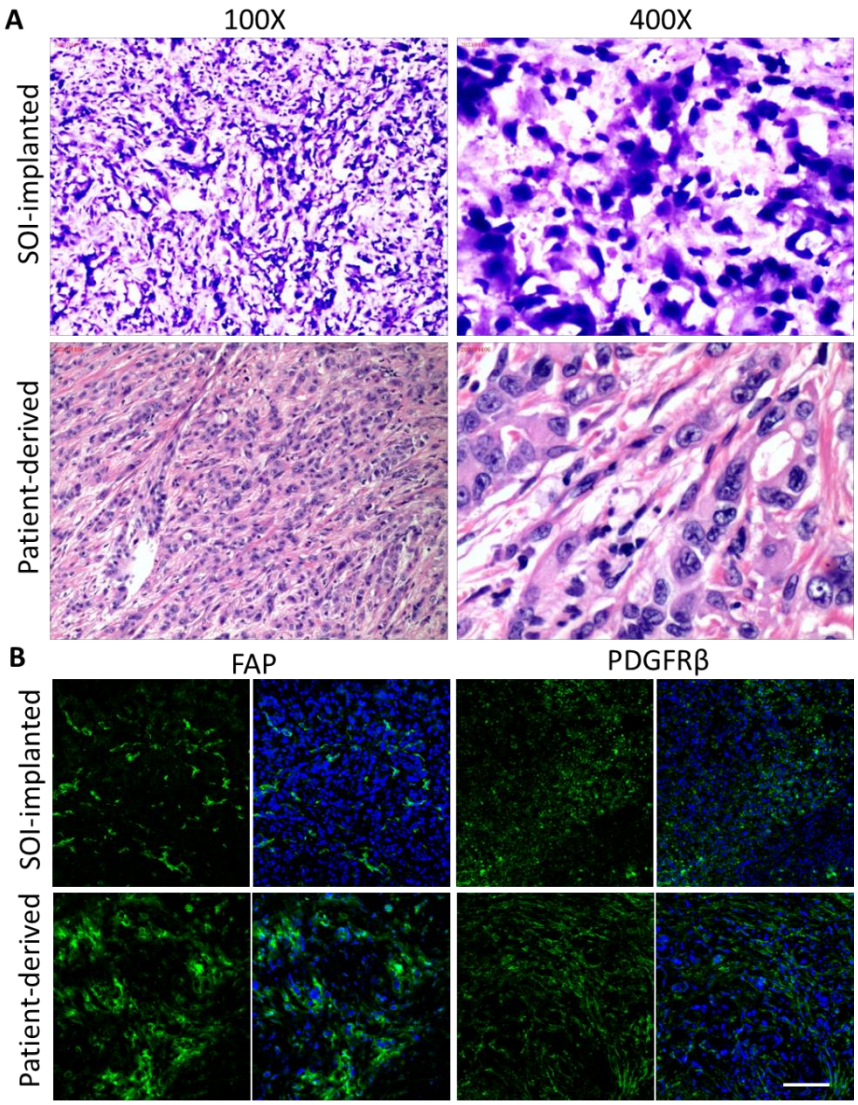

Figure S8. Comparison of the orthotopic PDAC and patient-derived pancreatic cancer tissues. (A) SOI-implanted model showed similar poorly differentiated pancreatic adenocarcinoma structure resembling clinical PDAC, as clarified by a pathologist in Hunan Cancer Hospital. SOI-implanted tumors were prepared in OCT block, whereas the patient-derived cancer tissues were processed in paraffin blocks, which displayed good morphology. (B) Contiguous sections were stained with fibroblast activation protein (FAP) or platelet-derived growth factor receptor β (PDGFR-β) antibody, and nuclei were stained with DAPI (blue), scale bar = 100 μm.

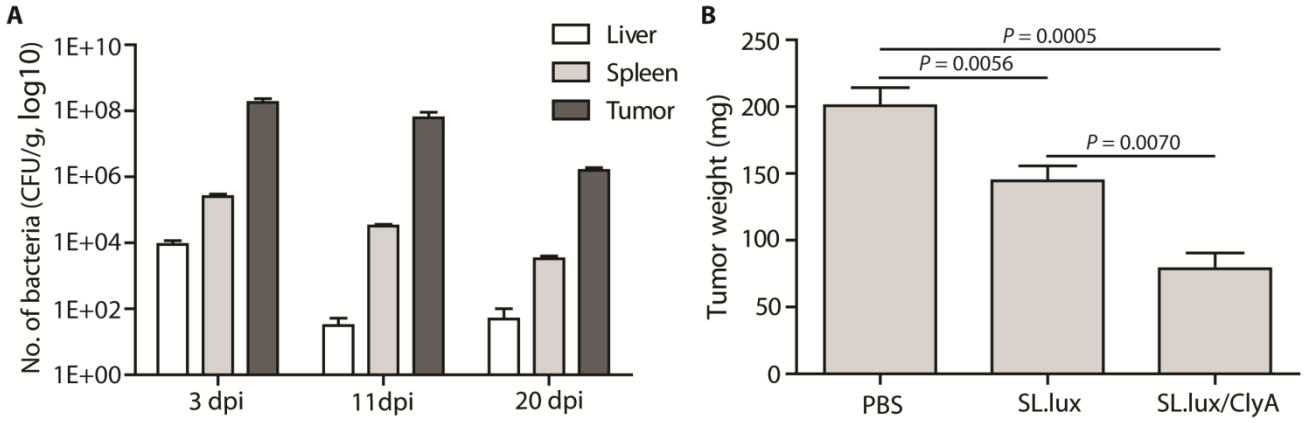

Figure S9. Anticancer activity in the orthotopic pancreatic cancer model. Mice harboring SOI-implanted cancer fragments (AsPC-1/Fluc) were injected intravenously with 3.0×10^7 CFU engineered SL^{lux}, $SL^{lux/ClyA}$, or PBS. (A) Quantification of bacteria in the liver, spleen, and tumor at 3, 11, and 20 days post-bacterial infection (n = 8 mice per group for each time point). (B) Primary tumor weight at Day 22 post-surgical implantation (7 dpi; n = 9 mice per group).

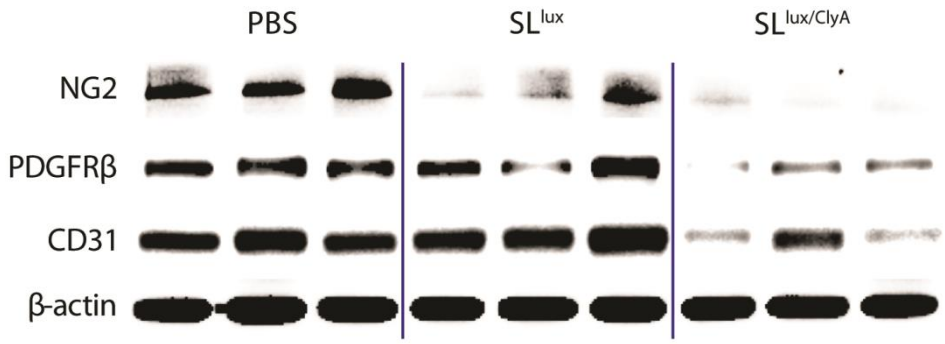

Figure S10. Stromal cell changes after treatment with ClyA-expressing bacteria. Samples were collected at 5 days post-bacterial infection (3.0×10^7 CFU, 48 hours after ClyA induction) from AsPC-1 mice. Expression of stromal cell markers was examined by Western blot analysis. NG2: Neural/glial antigen 2; PDGFRβ: Platelet-derived growth factor receptor β; CD31: Cluster of differentiation 31. Data are representative of at least two independent experiments.

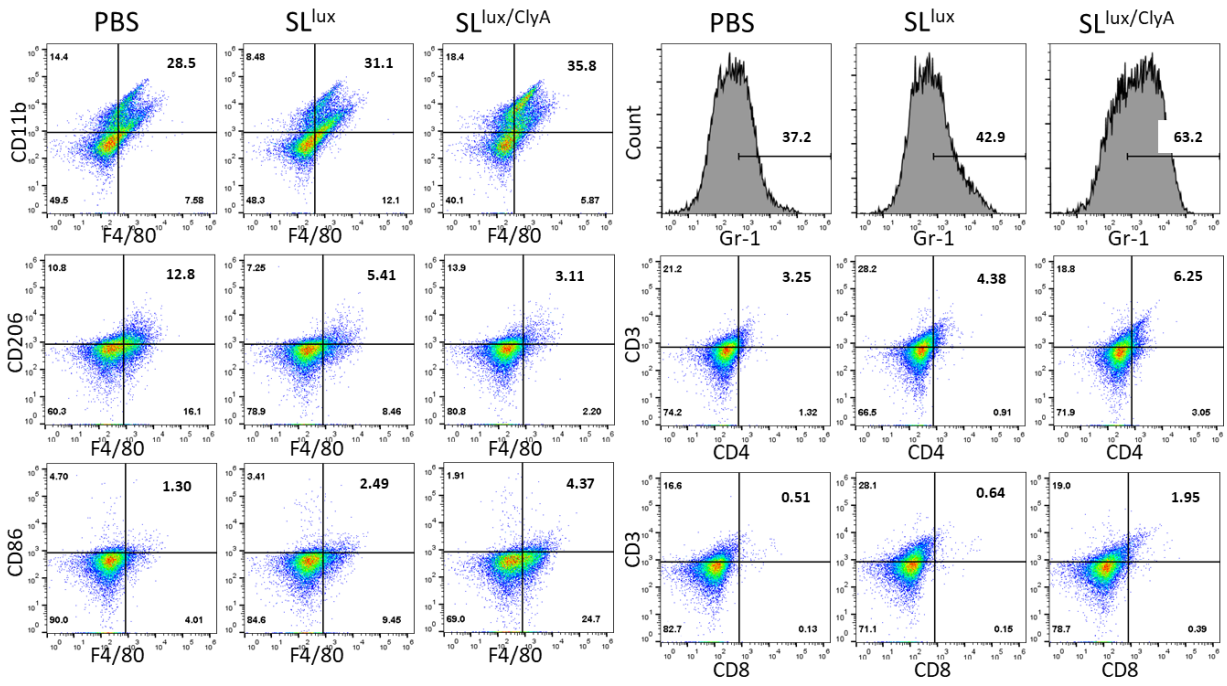

Figure S11. Immune cell analysis in tumor microenvironments. Single-cell suspensions from Pan02 tumors were prepared by incubating removed tumor pieces in 1.0 mg/ml collagenase D (Roche) and 50 µg/ml DNase I (Roche) for 45 min at 37 C, followed by passing through a 40 µm cell strainer. Samples were incubated with specific fluorochrome-labeled antibodies (Table S2) at 4 C for 30 min. At least 20,000 events were analyzed using a FACSCalibur flow cytometer (BD Biosciences). Data were analyzed using FlowJo (TreeStar) software. The analysis gate was set on the basis of isotype plots. Representative data with two independent experiments (n = 3). Macrophage, $CD11b^{+}F4/80^{+}$; M2-type macrophage, $F4/80^{+}$ $CD206^{+}$; M1-type macrophage, $F4/80^{+}$ $CD86^{+}$; Neutrophil, $Gr\text{-}1^{+}$; $CD4^{+}$ T cell, $CD3^{+}CD4^{+}$; $CD8^{+}$ T cell, $CD3^{+}CD8a^{+}$.

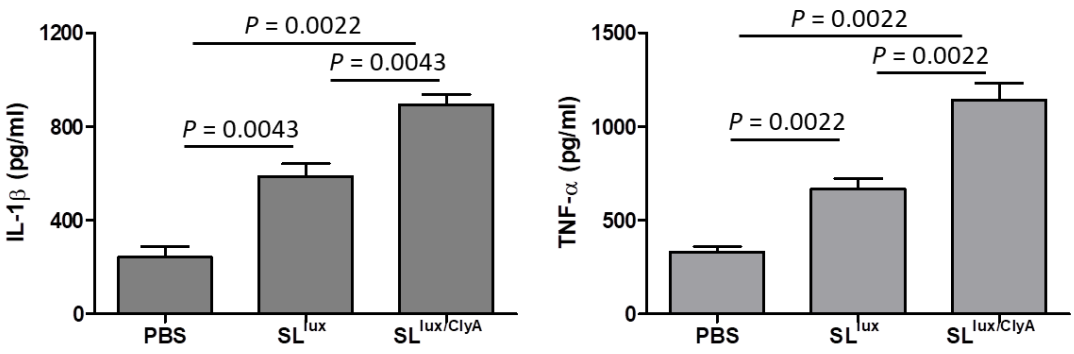

Figure S12. Detection of inflammatory cytokines in tumor tissues. Tumor tissues (n = 6 mice/group) were isolated from Pan02 tumor-bearing mice at 48 h after L-arabinose induction on day 5 post-bacterial infection. Cytokines were detected with IL-1β and TNF-α ELISA kits (eBioscience).

Table S1. Bacterial strains and plasmids used in the study

Strains/plasmids	Relevant genotype	Reference	Injection dose
S. typhimurium ΔppGpp (SL)	Δ*relA*, Δ*spoT*	24	1.0×10^7 CFU/mouse
S. typhimurium ΔppGpp lux (SL^{lux})	Δ*relA*, Δ*spoT*, lux operon	28	3.0×10^7 CFU/mouse
pBAD-Empty	Control vector	15	
pBAD-ClyA	ClyA-encoding	28	

CFU: colony-forming units.

Table S2. Antibodies used in the study

Antibody name	Antibody description	Company/Catalog no.	Remark
Rabbit anti-ClyA polyclonal antibody	Rabbit anti-ClyA	Yeongjin Hong Chonnam National Univ.	**Primary Ab**
Goat anti-*Salmonella* polyclonal antibody	Anti-*Salmonella*	GenWay Biotech/ GWB-AB2632	
β-actin (C4)	Mouse anti-β-actin	Santa Cruz Biotechnology /SC-47778	
Rabbit anti-NG2 chondroitin sulfate proteoglycan	Rabbit anti-NG2	Millipore /AB5320	
Anti-PDGF receptor beta antibody	Rabbit anti-PDGFRβ	Abcam/ab32570	
Anti-CD31 antibody	Rabbit anti-CD31	Abcam/ab28364	
Rat anti-mouse F4/80 (A3-1)	Rat anti-mouse F4/80	AbD Serotec/MCA497GA	
Neutrophil marker (6A608)	Rat mAb anti-mouse neutrophil	Santa Cruz Biotechnology /SC-71674	
Anti-CD4 antibody	Rat mAb anti-mouse CD4	Invitrogen/14-0041	
Anti-CD8a antibody	Rat mAb anti-mouse CD8a	Invitrogen/14-0081	
FAP polyclonal antibody	Rabbit anti-FAP	Invitrogen/PA5-99458	
PDGFRβ monoclonal antibody (G.290.3)	Rabbit anti-PDGFRβ	Invitrogen/MA5-15143	
Peroxidase-conjugated rabbit anti-mouse immunoglobulin	Rabbit anti-mouse	Dako/P0260	**Secondary Ab**
Peroxidase-conjugated goat anti-Armenian hamster immunoglobulin	Goat anti-hamster	Santa Cruz Biotechnology /SC-2443	
Peroxidase-conjugated goat anti-rabbit immunoglobulin	Goat anti-rabbit	Dako/P0448	
Alexa Fluor® 488 donkey anti-rat IgG (H+L) antibody	Donkey anti-rat	Invitrogen/A21208	
Alexa Fluor® 555 donkey anti-rabbit IgG (H+L) antibody	Donkey anti-rabbit	Invitrogen/A31572	
Alexa Fluor® 488 donkey anti-rabbit IgG (H+L) antibody	Donkey anti-rabbit	Invitrogen/A-21206	
Anti-mouse CD45 FITC	mAb (clone 30-F11)	eBioscience/11-0451	**FACS Ab**
Anti-mouse CD11b FITC	mAb (clone M1/70)	eBioscience/11-0112	
Anti-mouse F4/80 antigen PE	mAb (clone BM8)	Biolegend/123110	
Anti-mouse CD3 APC	mAb (clone 17A2)	eBioscience/17-0032	
Anti-mouse CD4 FITC	mAb (clone GK1.5)	eBioscience/11-0041	
Anti-mouse CD8a FITC	mAb (clone 53-6.7)	eBioscience/12-0081	
Anti-mouse Ly-6G (Gr-1) PE	mAb (clone RB6-8C5)	eBioscience/12-5931	
Anti-mouse CD86 (B7-2) APC	mAb (clone GL1)	eBioscience/17-0862	
APC anti-mouse CD206 (MMR)	mAb (clone C068C2)	BioLegend/141708	